# On the formation of cloud and precipitation systems under undisturbed conditions during TAMEX

*Ching-Sen Chen and Yuet-on E. Chan*

*Institute of Atmospheric Physics, National Central University, Chung-Li, Taiwan, R.O.C.*

## 1. Introduction

Mountains act as a heat and moisture source that can influence the formation of precipitation systems. Mountains can also disturb the prevailing wind and produce a divergence/convergence pattern as well as a lifting effect. These phenomina also affect the occurrence of precipitation systems. Kuo and Orville (1973) studied mountain storms over the Black Hills in South Dakota, U.S.A. They found that the prevailing wind could affect the position of the formation of such storms. Storms formed upstream and downstream of the mountainous area in the afternoon. Karr and Wooten (1976) analyzed radar echoes over the Rocky Mountains. They found that mountain "hot spots" were favorable for the formation of radar echo. Banta and Schaaf (1987) used satellite data to trace where mountain thunderstorms initially formed and found that that occured only on lee side. The "lee side convergence zone" as a favorable place for the formation of cumulus clouds has also been proposed by Banta (1984).

As mountains occupy so much of the land-mass of Taiwan island (Fig. 1), its effects on the formation of mountain storms is very important. Liao and Chen (1984) presented two cases where storms formed in mountainous areas in the afternoon and then moved toward the Taiwan strait under a southeasterly wind. In 1987 the Taiwan Area Mesoscale Experiment (TAMEX, Kuo and Chen, 1990) was held in Taiwan. One of its objectives was to study orographic effects on the formation of precipitation systems. Johnson and Bresch (1991) found (May 24, 25 and 26, 1987) from TAMEX'S data that precipitation systems formed predominantly between the 100- and 500-m elevations in the foothills of the interior mountains rather than over the higher elevations farther inland during undisturbed periods (Fig. 2). Chen et al. (1991) studied a mountainous storm which formed in a mountain slope area in the afternoon in northern Taiwan which then moved eastward on 7 June 1987. This system dumped more than 100 mm of precipitation at some stations in only a few hours (Fig. 2). The maximum reflectivity was over 50 dBZ along the steep slope and near the mountain peak. On June 19 and 20, 1987 significant rainfall was also observed (Fig. 2) when a Pacific high prcessure area was present over Taiwan. One common feature was that most of rainfall occurred in the afternoon for these six days (May 24, 25, 26, June 7, 19 and 20) (Fig. 3) under the influence of the Pacific high pressure area (Fig. 4). However wind profiles around Taiwan island were not necessarily the same. To understand if any relationship between the wind profiles in the upsteam direction of Taiwan island and the formation of a cloud and precipitation system is good for forecasting the occurrence of cloud and precipitation systems, we will present the observation results in section 2. Some simulation results regarding the formation of cloud and precipitation systems under the influence of the observated wind in an upstream direction from Taiwan by a three dimentional numerical model will be given in section 3. A brief summary is provided in section 4.

## 2. Data Analysis

Figure 4 presents the synoptic-scale surface map at 0800 LST(0000 UTC) on May 24, 25, 26, and June 7, 19 and 20 respectively. Taiwan was situated on the western side of a Pacific High pressure system in general. However the detailed position was not necessarily the same day by day. The Pacific High pressure system continually moved toward southern China from May 24 to 26. Thus the wind direction

shifted from 230° (May 24, 25) to 250° (May 26) between 2 to 3 km height (Fig. 5). On June 7, the Pacific High pressure retreated eastward and the wind was nearly westerly (254°) (Fig. 5). From June 19 to 20 a Pacific High moved west and the wind direction changed from 163° (June 19) to 188° (June 20) (Fig. 5) between 2 to 3 km in height.

Under the influence of insulation when the Pacific High pressure was present, the on-shore flow and upslope wind was very evident over Taiwan island. Fig. 6 presents one example at 1200 LST on 20 June. Wind was from the south or the southwest in the remote islands, however the on-shore flow was very evident in northern and central Taiwan. Besides upslope wind occurred in the sloped area in northern Taiwan. Johnson and Bresch (1991) also indicated that the sea-breeze onset was typically around 0900 LST on May 24, 25 and 26. The level of free convection (LFC) was near or less than 1 km in height in the afternoon (Fig. 7). Most of rainfall occurred in the afternoon (Fig. 3), in the mountainous and sloped area (Fig. 2) but not along the coastal area. Thus the topography was very important. Lifting due to the interaction of an on-shore flow and upslope wind with topographical or other mechanisms was expected to help air parcels at the low level to rise and form cloud and rain. Johnson and Bresch proposed that the inflowing sea-breeze, first an abrupt rise in the topography, thus causing the formation of precipitation along a sloped area.

The precipitible water content was 47 kg $m^{-2}$ on May 26. It were greater than 52 kg $m^{-2}$ in the other five cases. Thus the rainfall amount was least on May 26 among these six cases. On June 19 most of the rainfall took place over western and northwestern Taiwan when wind at the 2 to 3 km height was from south-south east. The rainfall occured in the down stream area of Taiwan's topography. In the other five cases rainfall also occured in the downstream area. However on May 24, 25, 26 and June 7 rainfall also took place in an upstream areas as well as in a downstream area. Thus the wind direction as well as the topography was also important for the occurrence of a cloud and precipitation system.

## 3. Model Structure

The numerical model used in this study was a finite-difference approximation of the elastic, non-hydrostatic equations governing atmospheric motion. This model utilized the compressible equations which were efficiently solved by separating out sound wave terms and integrating them with a smaller time step than that used for the convective processes, in order to maintain computational stability. The predicted variables included horizontal and vertical velocities, pressure, potential temperature ($\theta$), the mixing ratio of water vapor ($q_v$), of cloud water ($q_c$) and of rainwater ($q_r$). Cloud water and rainwater growth were parameterized in the manner suggested by Kessler (1969), but with the coefficients used by Klemp and Wilhelmson (1978). The subgrid scale parameterization used in this study followed Lilly's formulation (1962) which depended on the relative strengths of stratification and shear.

The boundary conditions of the velocity components for the upper and lower boundaries were assumed to have zero normal velocity and zero normal velocity gradient conditions for the horizontal velocities. There was also no normal gradient for $\theta$, $q_v$, $q_c$, and $q_r$ at the boundaries. In the upper half of the model domain, a region of Rayleigh friction and Newtonian cooling were applied to the perturbation velocities and $\theta$. The lateral boundary conditions were assumed to have no horizontal gradient at the inflow boundaries, but Orlanski (1976) type conditions were employed for the horizontal velocities of the outflow boundaries.

The numerical scheme used in the model was similar to that of Durran and Klemp (1982). The model domain was 400 km × 800 km × 10 km. The horizontal grid interval was 10 km and the vertical grid interval varies from 173 m near the surface to 642 m near the top. The big time step was 4 seconds and the small time step was 1 second. Smooth terrain with mountain peak 3 km in height was assumed in the model (Fig. 8).

## 4. Simulation results

The initial temperature and moisture profile used in the model are shown in Fig. 7 while the initial wind profiles are presented in Fig. 5. To avoid the big shock in the model, the wind speed was initially made to be zero everywhere in the model and then slowly increased in the first three hours to its environmental value assumed in the model. Then we let the model run for another hour. At 4 hours of simulation time surface heating was activated on the lowest level over the land for another two hours. The heating added to the model was similar to that in Banta, (1986). During this time the surface temperature could increase about 2° K over the plain in the model, which was close to the observed value for the maximum temperature variation at 1300 LST in these six cases.

Fig. 9 shows the streamline at 4 hr for the May 24 case. Stippled and hatched areas in Fig. 9 represent the maximum cloud water and rainwater, respectively, in a vertical column after 6 hr of the simulation time (2 hours after surface heating is activated). Cloud and rainwater occurred in the upslope area (western side of Taiwan) and mountainous areas where topographic lifting was evident (Fig. 9). The convergence areas in northeastern and southeastern Taiwan were also covered by cloud and rainwater. Upsloped wind could later enhance the convergence when heating was activated. The distribution of cloud and rainwater were basically similar to the cloud image (Fig. 3) and rainfall amount (Fig. 2). Figs. 10, 11, 12, 13 and 14 are for May 25 and 26, June 7, 19 and 20 respectively. In general cloud and rain occurred in the central mountain area where lifting and heating was evident. To the upstream side of the mountain where topographic lifting was obvious, cloud and rain systems could take place. On the downstream side of the mountain where convergence occurred, we could also find cloud and rain systems.

## 5. Conclusion

During Mei-Yu season when Pacific high pressure systems influence Taiwan, cloud and rain systems can form in mountain and sloped areas in the afternoon. On May 24 to 26, June 7, June 19 to 20, 1987, this phenominon occured as illustrated in Figs. 2 and 3. The level of free convection (LFC) was about 1 km in height in the afternoon. Thus lifting from topographical effects or other factors could help convection occur. Observational analysis and numerical simulation indicate that cloud and precipitation systems could occur in the central mountain area where lifting and heating were evident. On the upstream side of the mountain where topographic lifting was obvious, cloud and rain systems could take place. On the downstream side of the mountain where convergence occurred, we also could find cloud and rain systems.

**Acknowledgments** This research is supported by the National Science Council under Grant NSC-83-0202-M-008-040 and NSC-82-0618-M-008-082. The computer resources were supplied by the Institute of Atmospheric Physics and the Computer Center of National Central University.

### References

Banta, R. M., 1984: Daytime boundary-layer evolution over mountainous terrain. Part I : Observations of the dry circulations. *Mon. Wea. Rev.*, **112**, 340-356.

Banta, R. M., 1986: Daytime boundary-layer evolution over mountainous terrain. Part II : Observations of the dry circulations. *Mon. Wea. Rev.*, **114**, 1112-1130.

Banta, R. M., and C. B. Schaaf, 1977: Thunderstorm genesis zones in the Colorado Rocky Mountains as determined by traceback of geosynchronous satellite images. *Mon. Wea. Rev.*, **105**, 463-476.

Chen, C.-S., W.-S. Chen and Z. Deng, 1991: A study of a mountain-generated precipitation system in northern Taiwan during TAMEX IOP 8. *Mon. Wea. Rev.*, **119**, 2574-2606.

Durran, D. R., and J. B. Klemp, 1982: The effects of moisture on trapped mountain lee waves. *J. Atmos. Sci.* , **39** , 2490-2506.

Johnson, R. H. and J. F. Bresch, 1991: Diagnosed characteristics of Mei-Yu precipitation systems over Taiwan during the May-June 1987 TAMEX. *Mon. Wea. Rev.*, **120**, 2540-2557.

Karr, T. W. and R. L. Wooten, 1976: Summer radar echo distribution around Limon, Colorado. *Mon. Wea. Rev.*, **104**, 728-734.

Kessler, E., 1969: On the distribution and continuity of water substance in atmospheric circulation. *Meteor. Monogr.*, **32**, Am. Meteor. Soc., 84pp.

Klemp, J. B., and R. B. Wilhelmson, 1978: The simulation of three-dimensional convective storm dynamics. *J. Atmos. Sci.*, **35**, 1070-1096.

Kuo, J. T. and H. D. Orville, 1973: A radar climatology of summertime convective clouds in the Black Hills. *J. Appl. Meteor.*, **12**, 357-368.

Kuo, Y.-H., and G.T.-J. Chen, 1990: The Taiwan Area Mesoscale Experiment (TAMEX): An overview. *Bull. Amer. Meteor. Soc.* ,**71** , 488-503.

Liao, S. Y., and C. S. Chen, 1984: The preliminary study of organized radar echo of frontal system and summertime convective systems. *Proc. Natl. Sci. Counc.*, **A8**, 250-266.

Lilly, D. K., 1962: On the numerical simulation of buoyant convective. *Tellus*, **14**, 148-172.

Orlanski, I.,1976: A simple boundary condition for unbounded hyperbolic flow. *J. Computer Phys.*, **21**, 251-269.

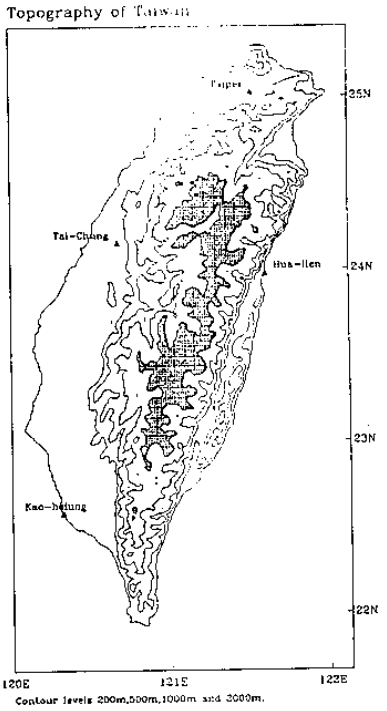


Fig. 1 The topography of Taiwan in meters.

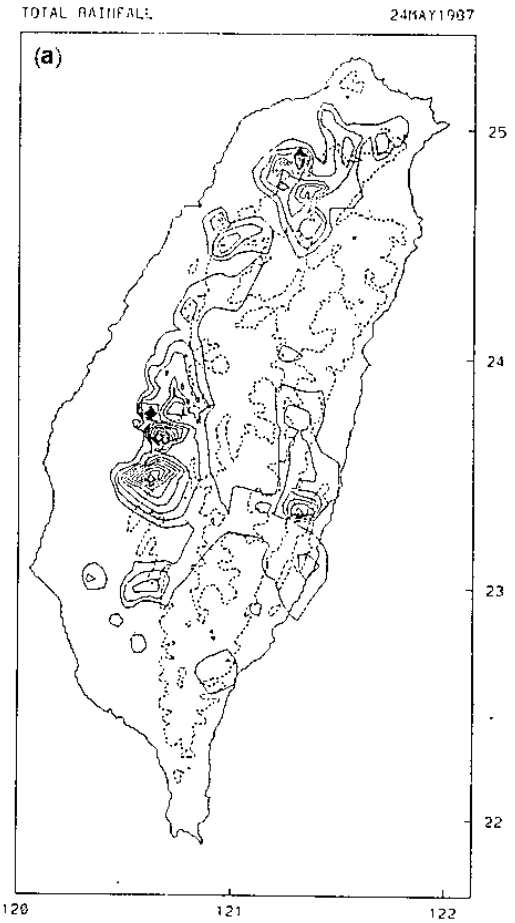


Fig. 2 The daily rainfall amount (mm) over Taiwan island on (a) May 24 (b) May 25 (c) May 26 (d) June 7 (e) June 19 (f) June 20, 1987. The contour intervals are 10 mm.

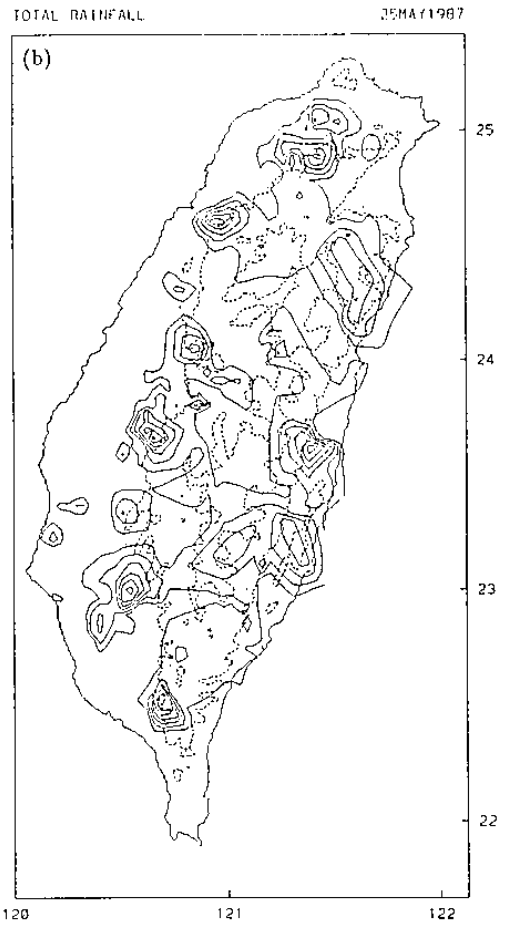
TOTAL RAINFALL
25MAY1987
(b)
25
24
23
22
120
121
122

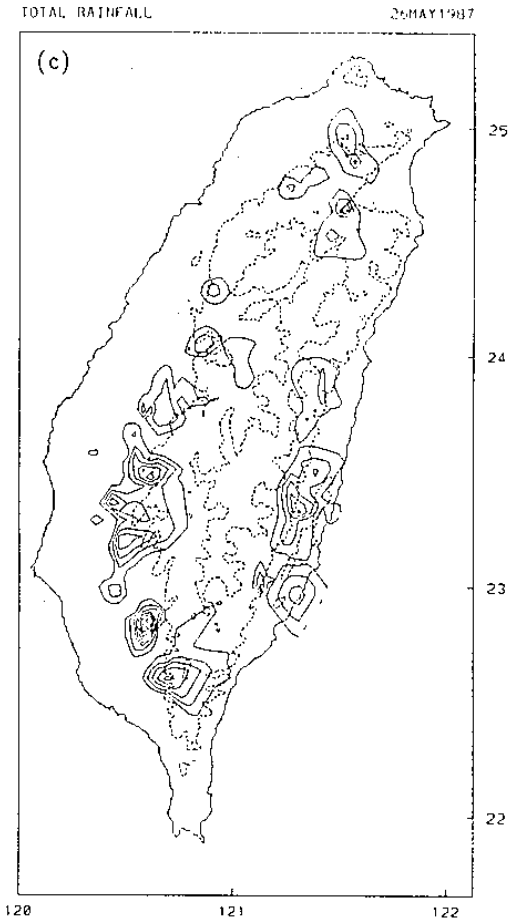
TOTAL RAINFALL
26MAY1987
(c)
25
24
23
22
120
121
122

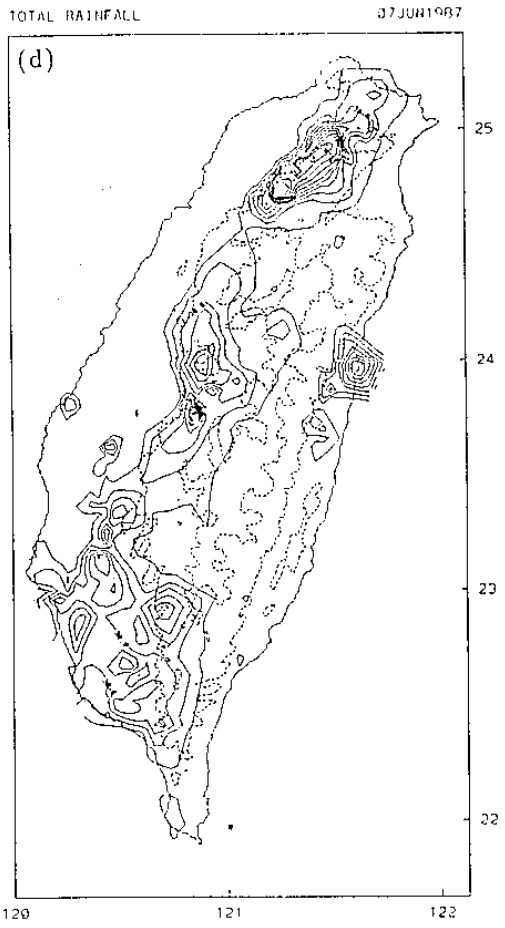
TOTAL RAINFALL
07JUN1987
(d)
25
24
23
22
120
121
122

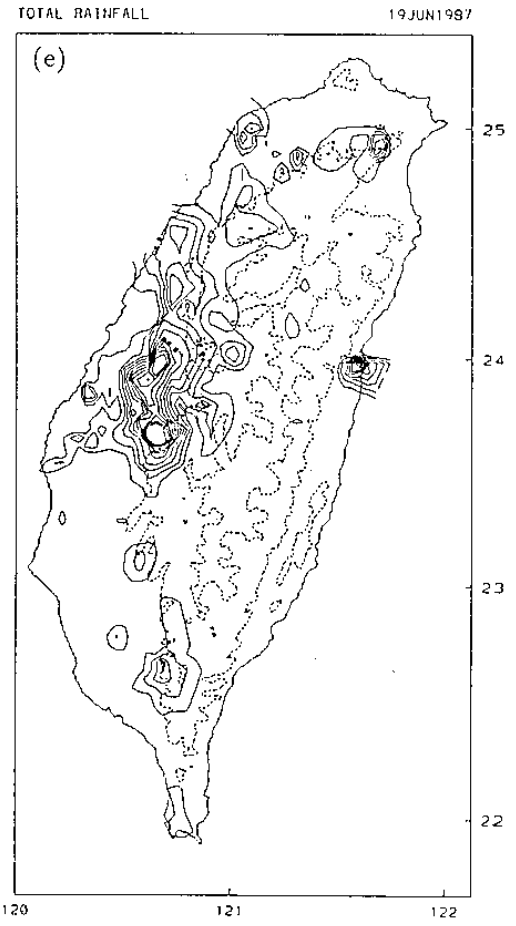
TOTAL RAINFALL
19JUN1987
(e)
25
24
23
22
120
121
122

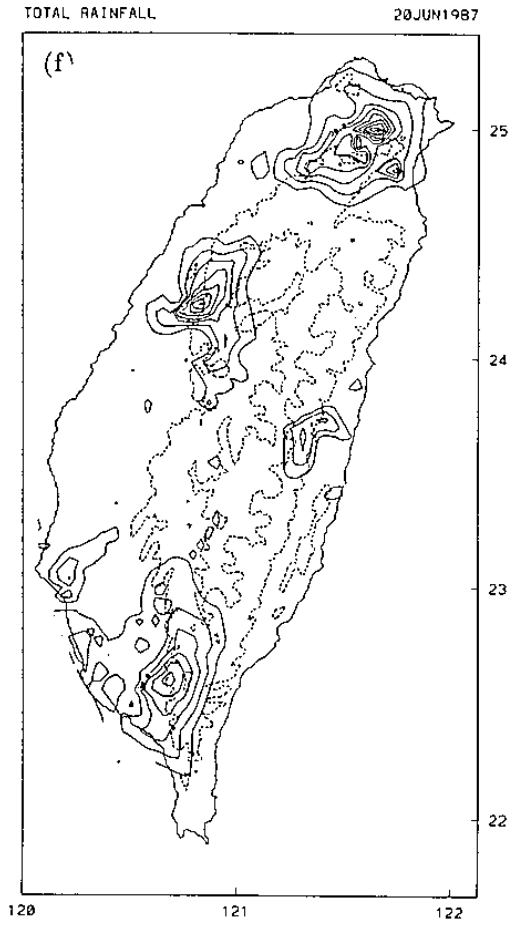


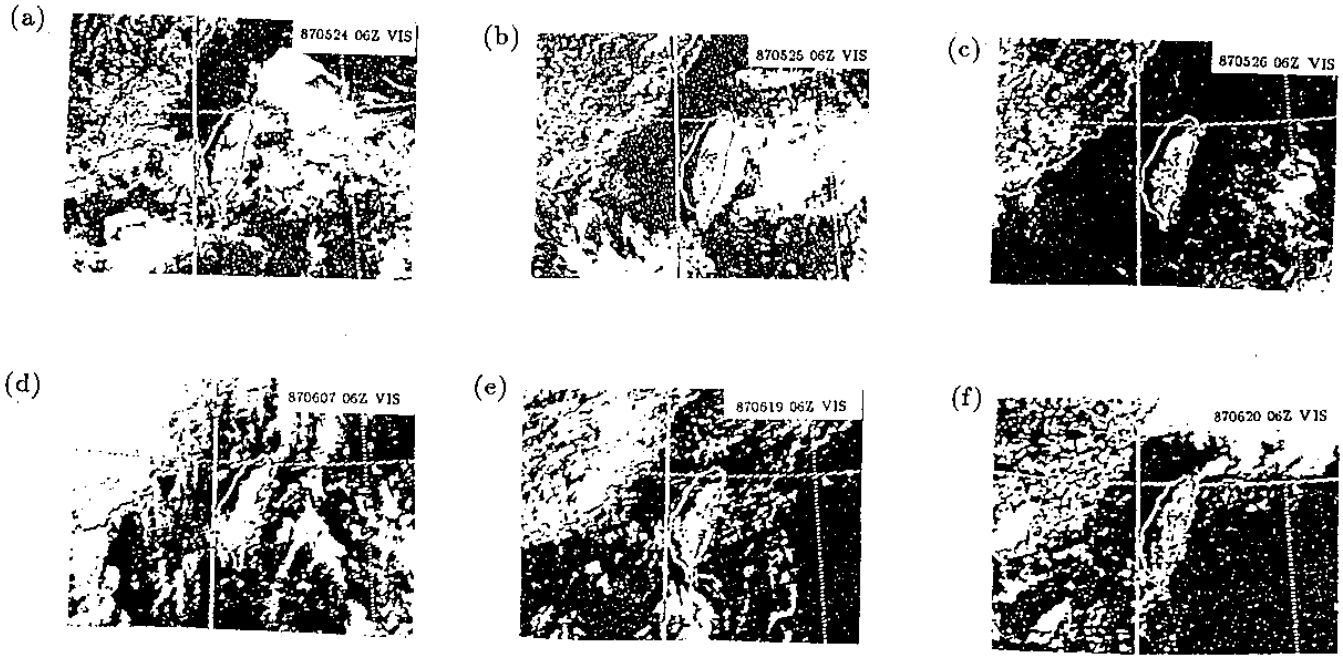


Fig. 3 Visible satellite images for 1400 LST (local standard time) for (a) May 24 (b) May 25 (c) May 26 (d) June 7 (e) June 19 (f) June 20, 1987.

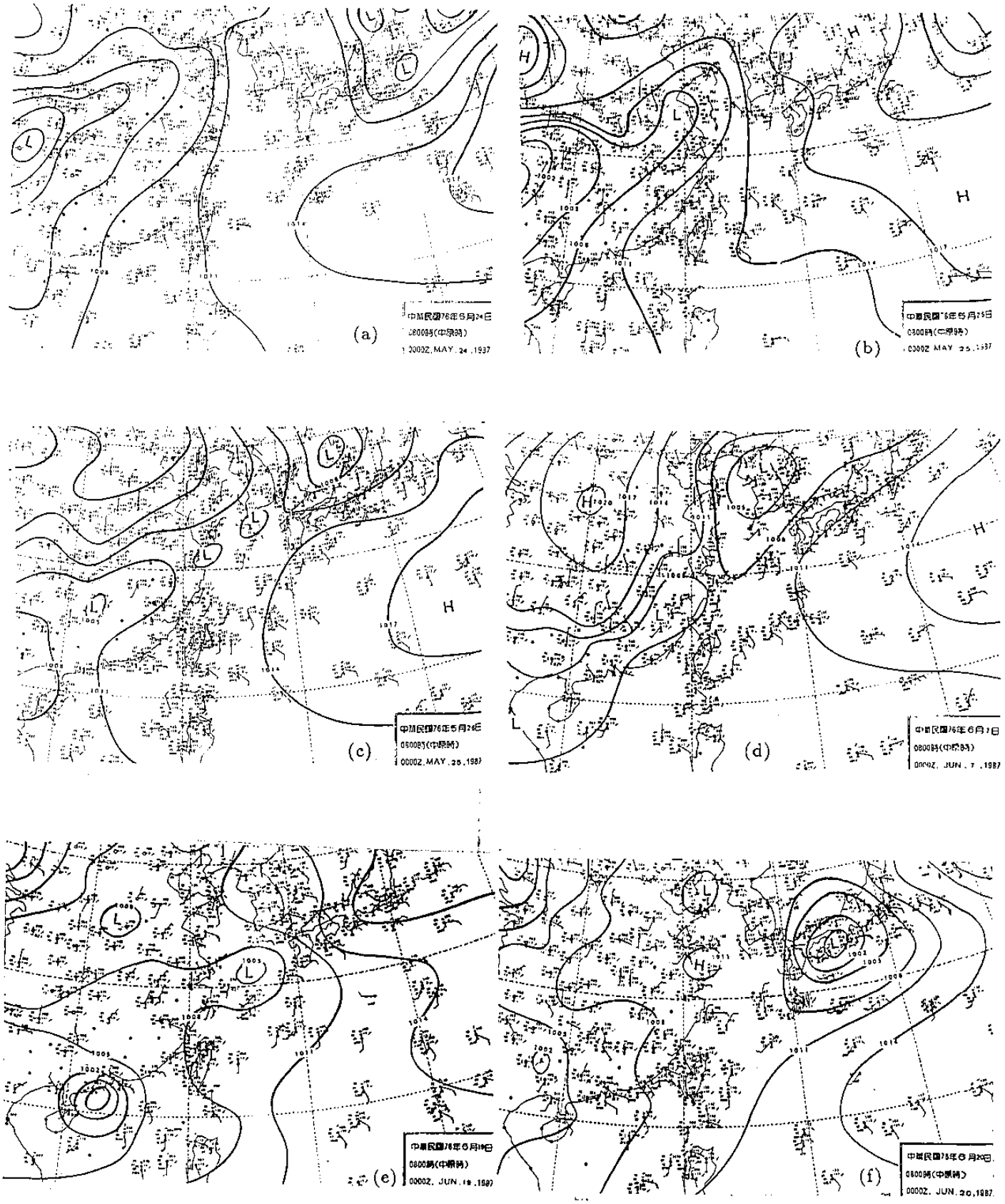


Fig. 4 Synoptic-scale surface map for (a) May 24 (b) May 25 (c) May 26 (d) June 7 (e) June 19 (f) June 20, 1987.

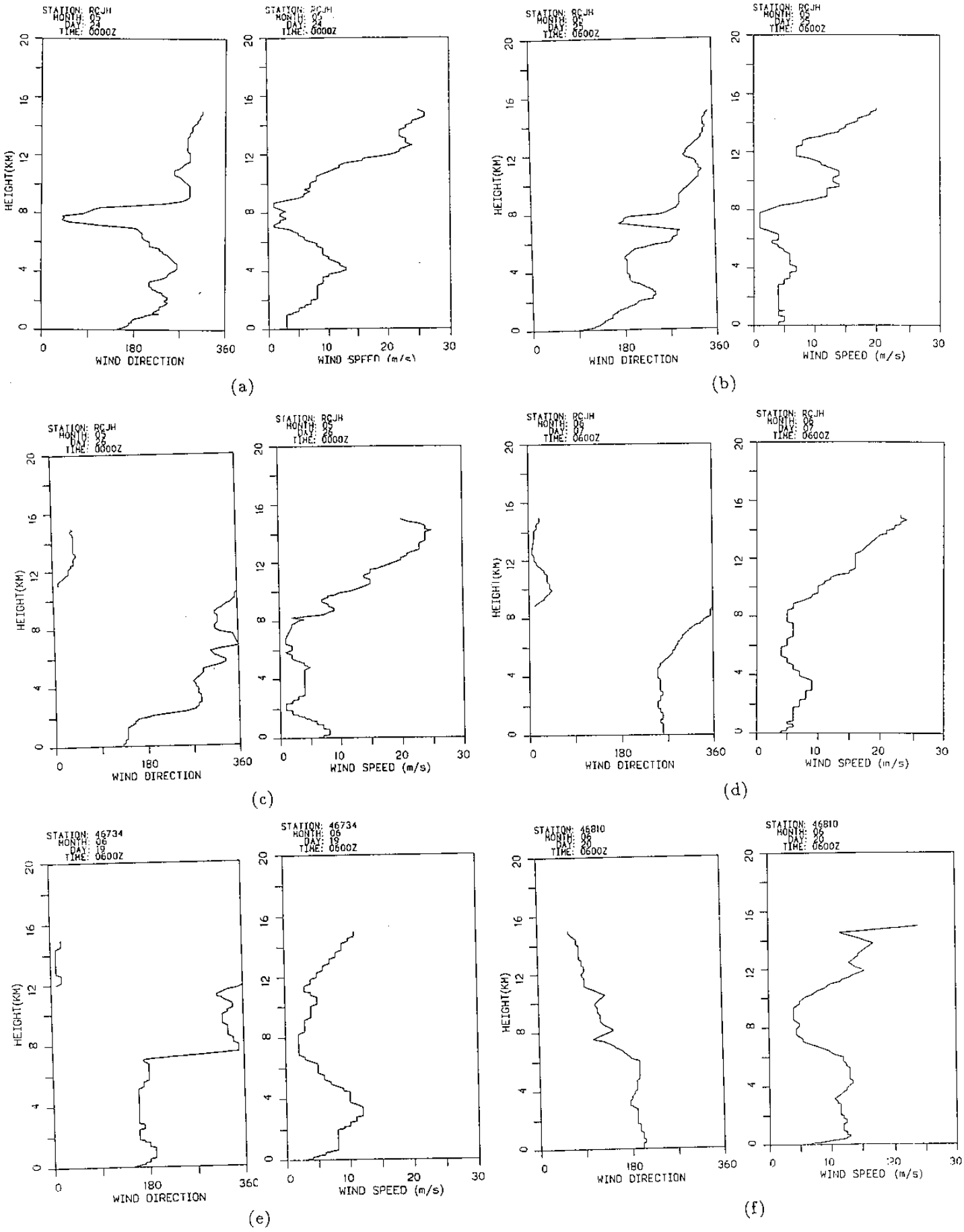


Fig. 5 The vertical profile of wind direction and speed over (a) Marine ship at 0800 LST, May 24, 1987 (b) Marine ship at 1400 LST, May 25, 1987 (c) Marine ship at 0800 LST, May 26, 1987 (d) Marine ship at 1400 LST, June 7, 1987 (e) Ma-Kung at 1400 LST, June 19, 1987 (f) Tung-Sha-Tao at 1400 LST, June 20, 1987

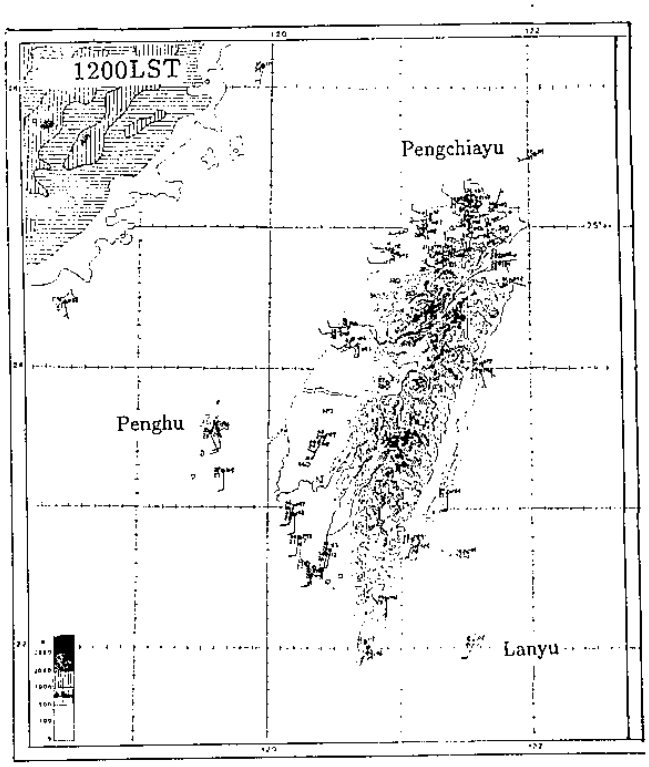


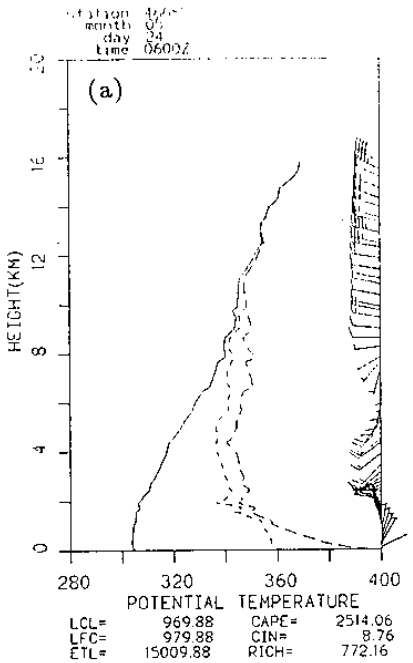


Fig. 6 Conventional meteorological variables on the surface for 1200 LST on June 20, 1987, in the Taiwan area.

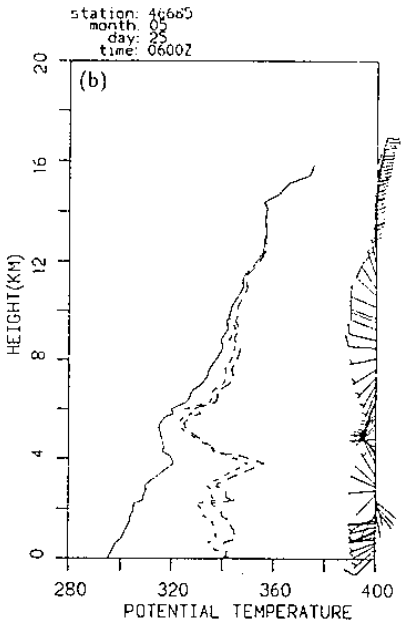


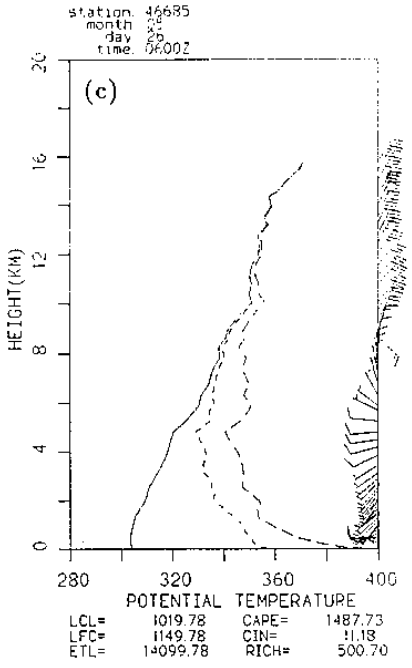


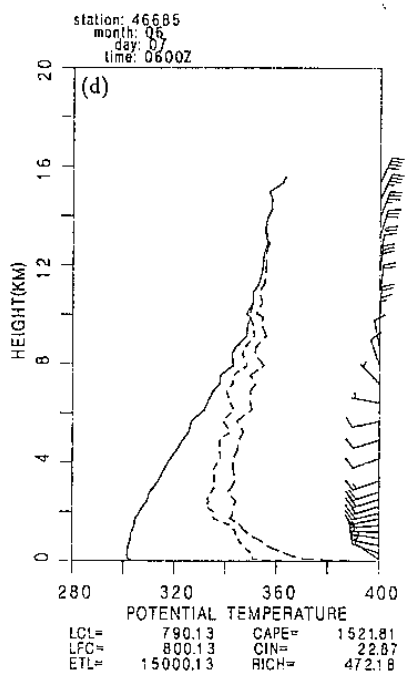

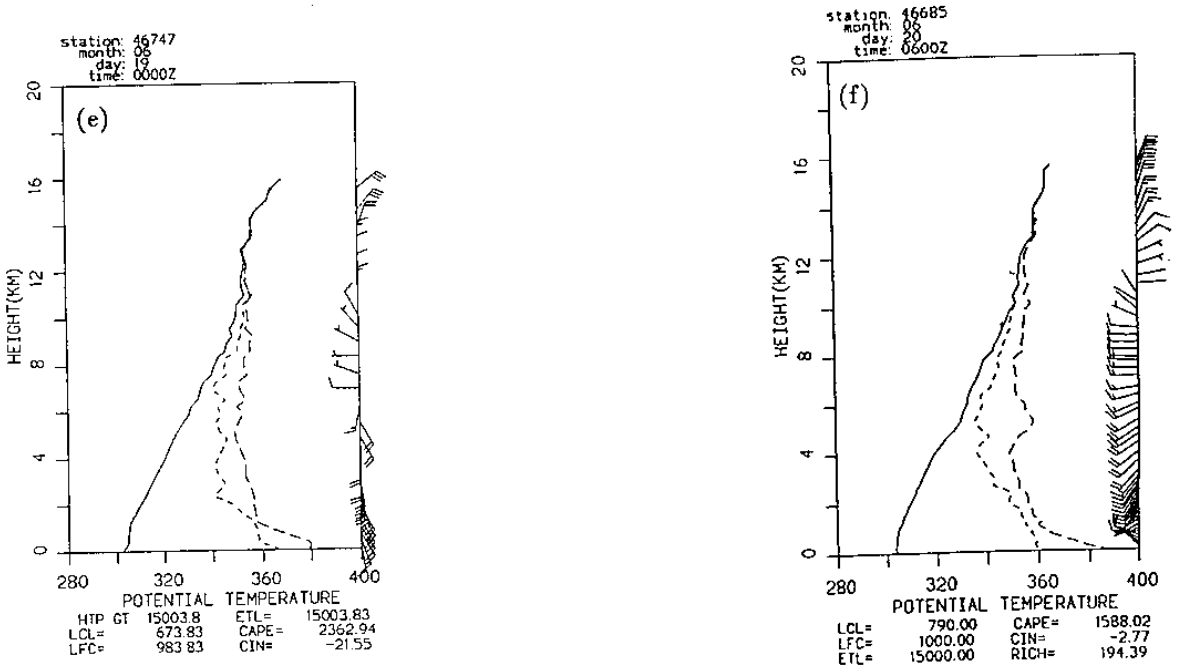


Fig. 7 The vertical profiles of potential temperature ($\theta$), equivalent potential temperature ($\theta_e$) and saturated equivalent temperature ($\theta_e^*$) at 1400 LST at Pan-chiao for (a) May 24 (b) May 25 (c) May 26 (d) June 7 (e) June 19 (f) June 20, 1987.

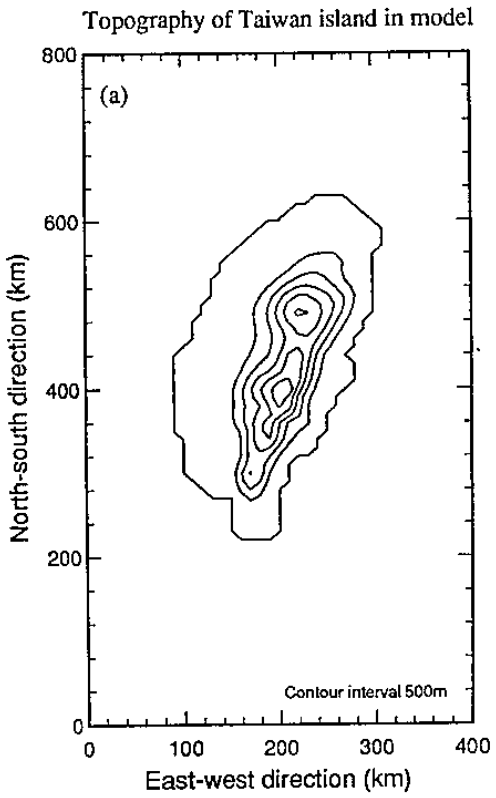


Fig. 8 The smooth terrain used in the model. Contours intervals are 500 m.

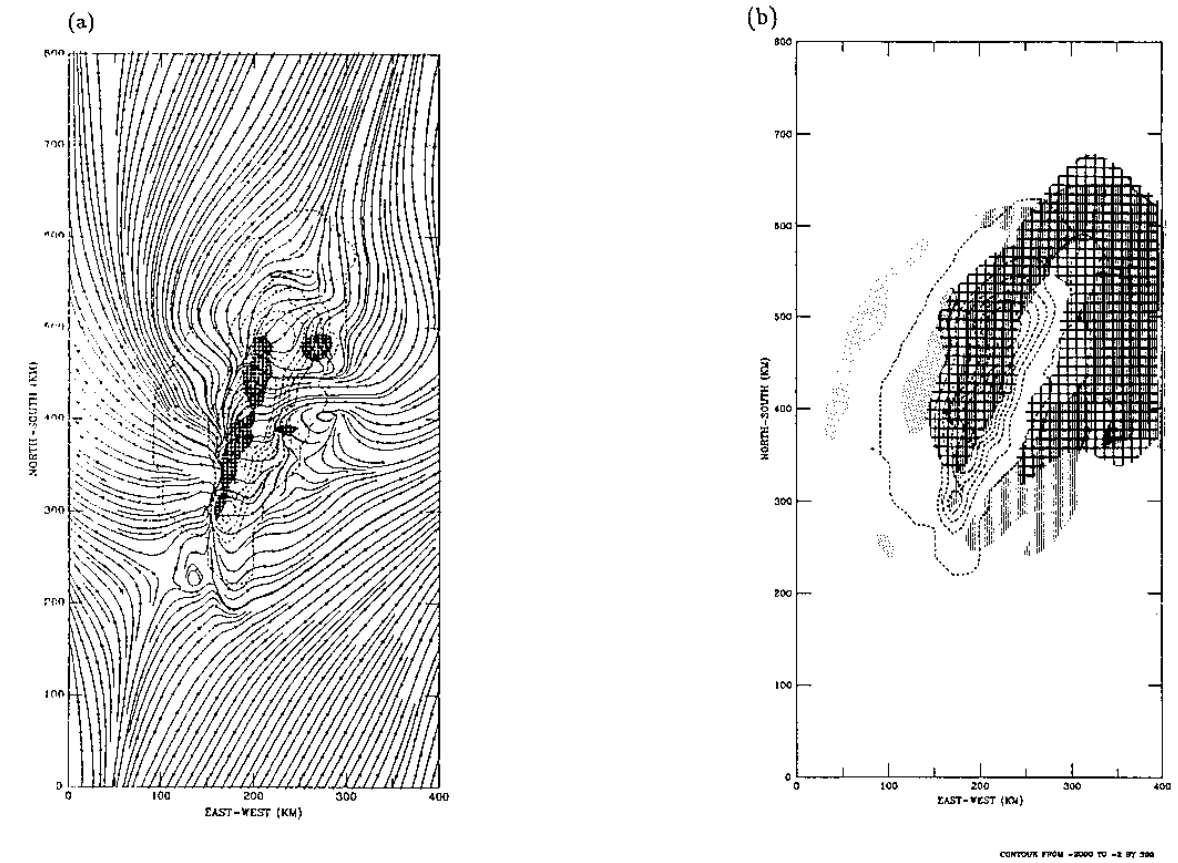


Fig. 9 (a) Surface streamline from model results at 4 hr for May 24, 1987. (b) Stipple areas denotes the maximum cloud water in the vertical column from model results (greater than 0.01 g $kg^{-1}$) and hatched areas represents the maximum rainwater in the vertical column from model results (greater than 1 g $kg^{-1}$) for May 24, 1987.

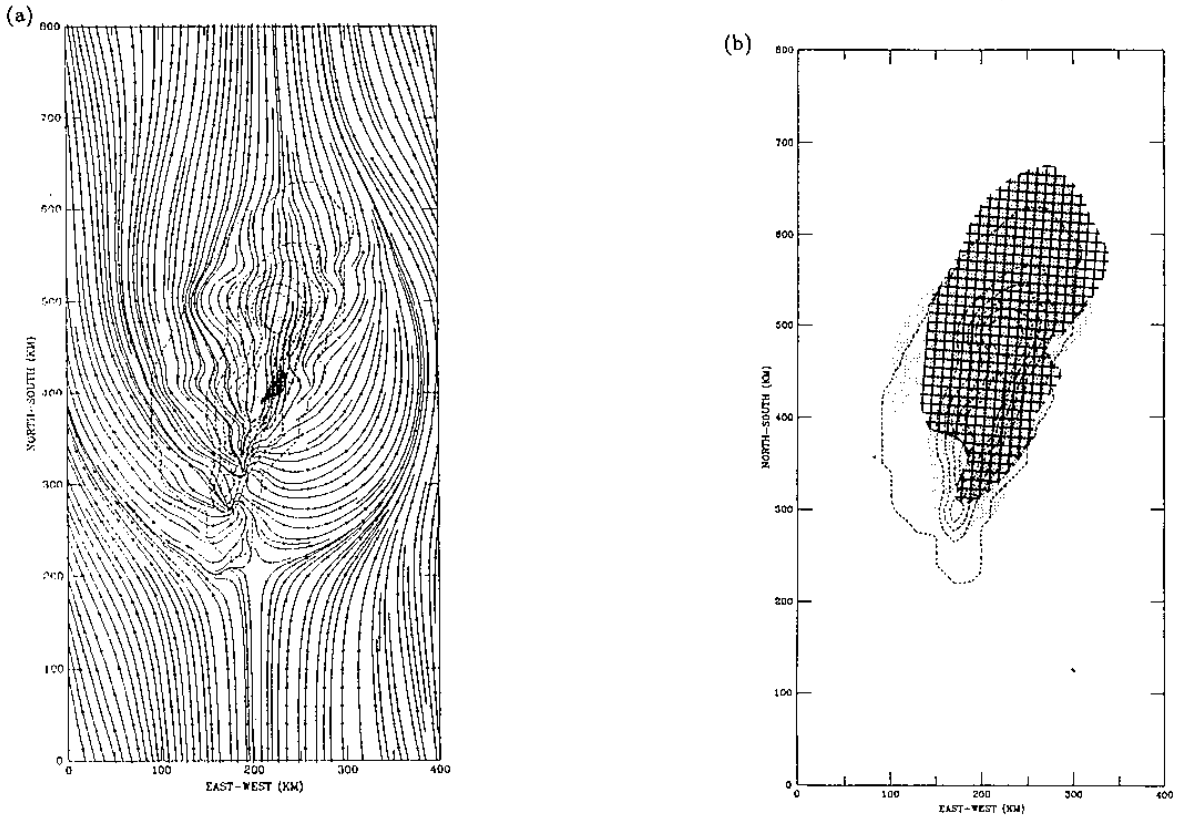


Fig. 10 Same as in Fig.9 but for May 25, 1987.

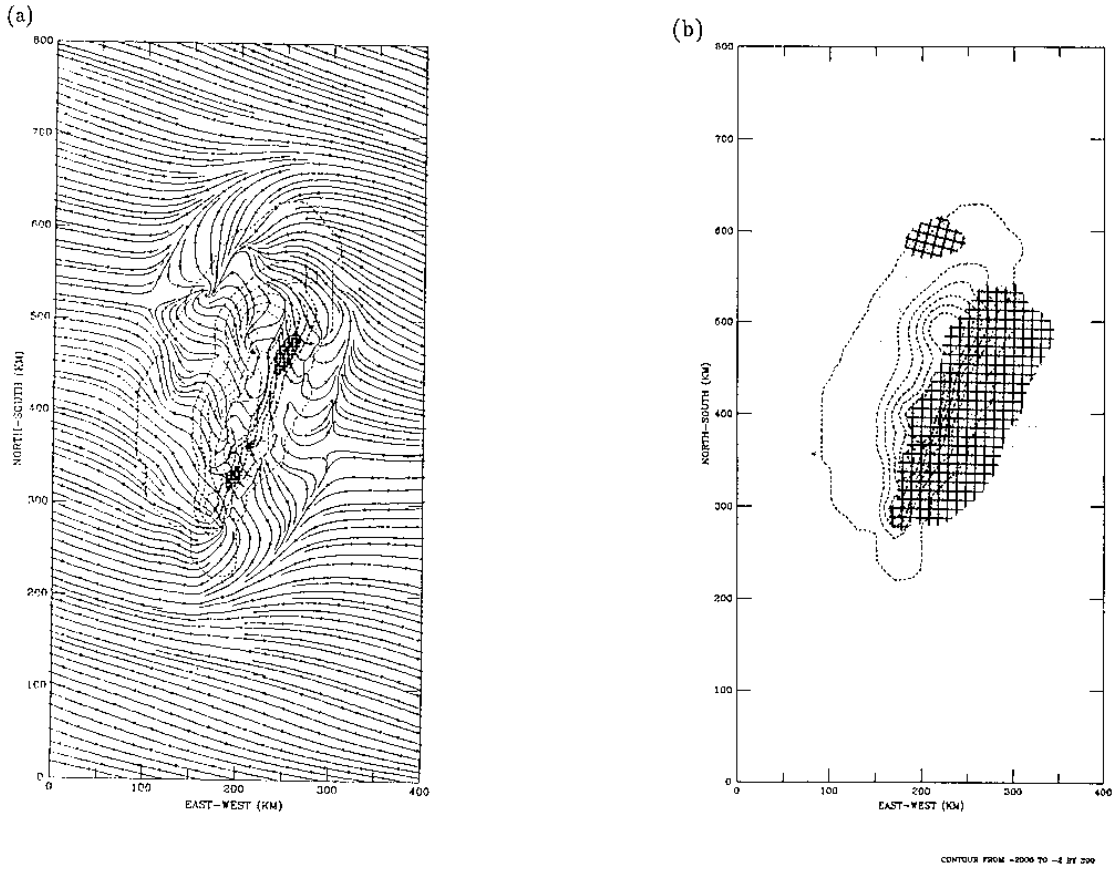


Fig. 11 Same as in Fig.9 but for May 26, 1987.

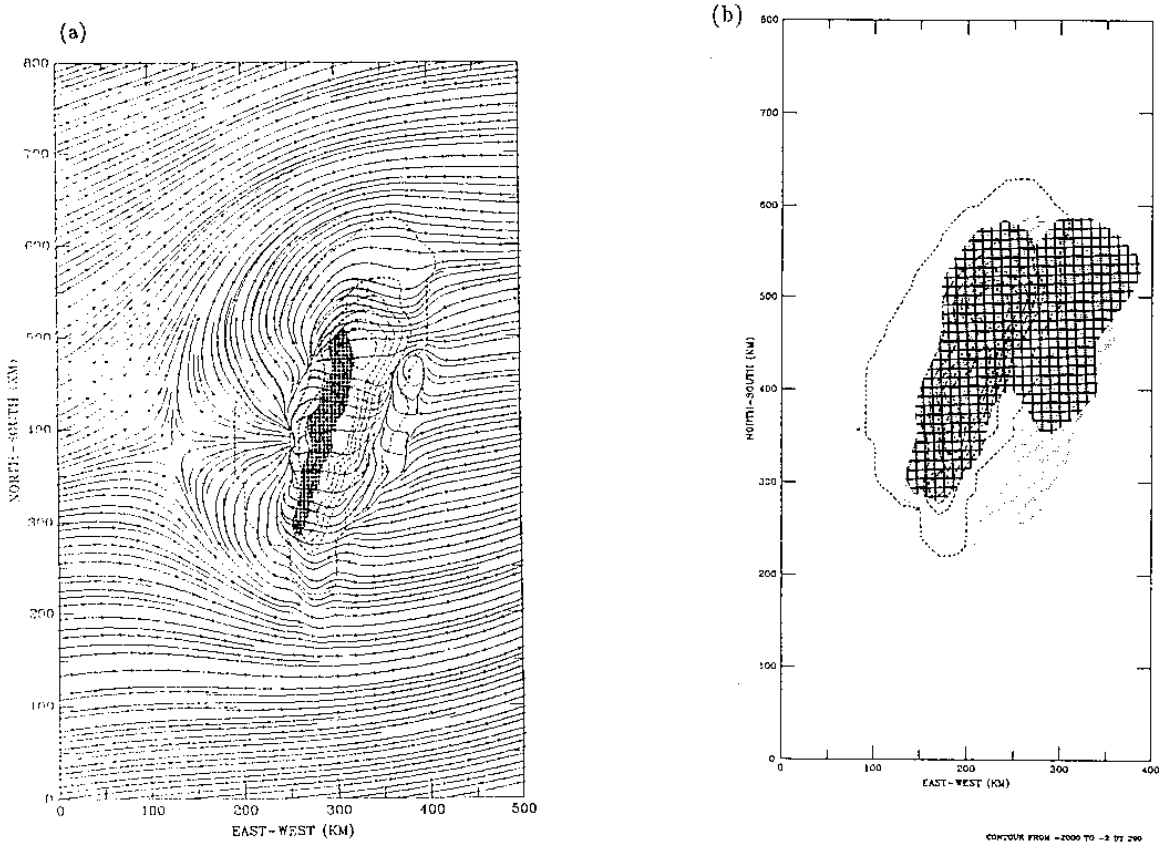


Fig. 12 Same as in Fig.9 but for June 7, 1987.

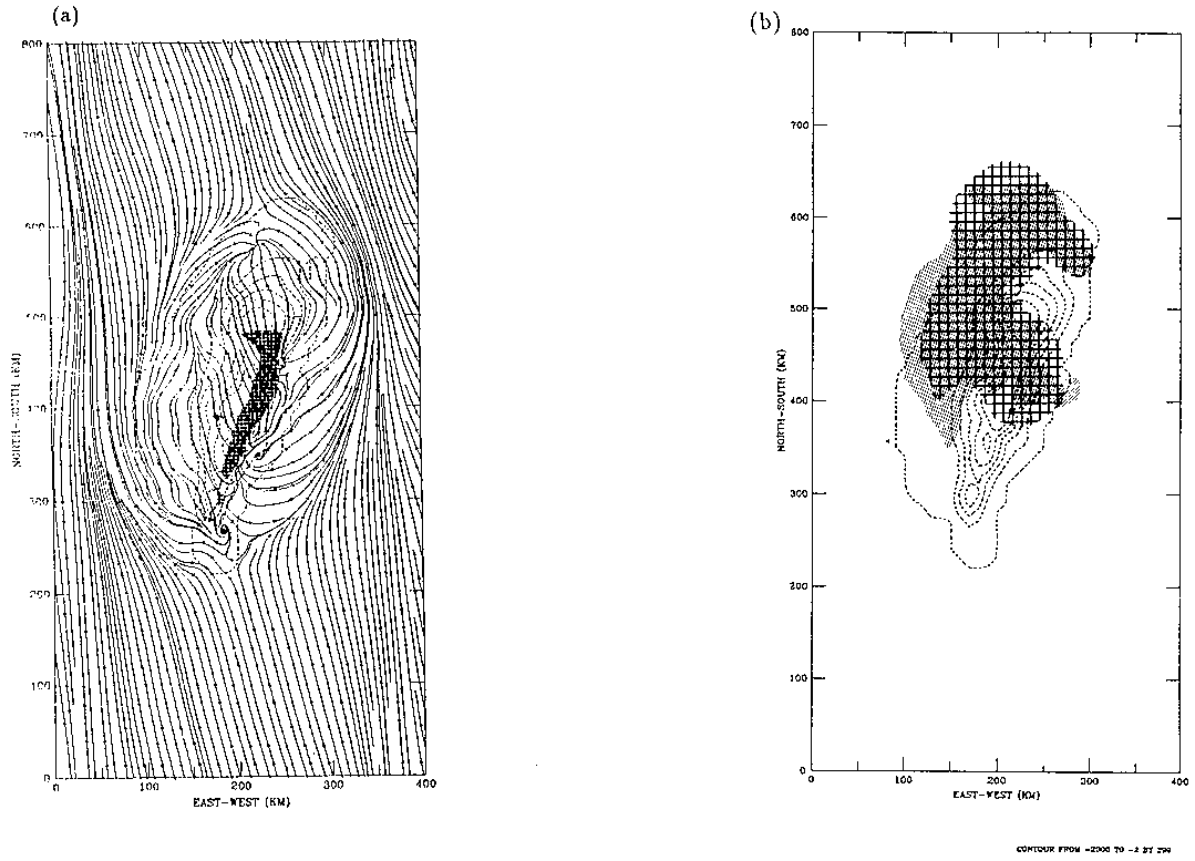


Fig. 13 Same as in Fig.9 but for June 19, 1987.

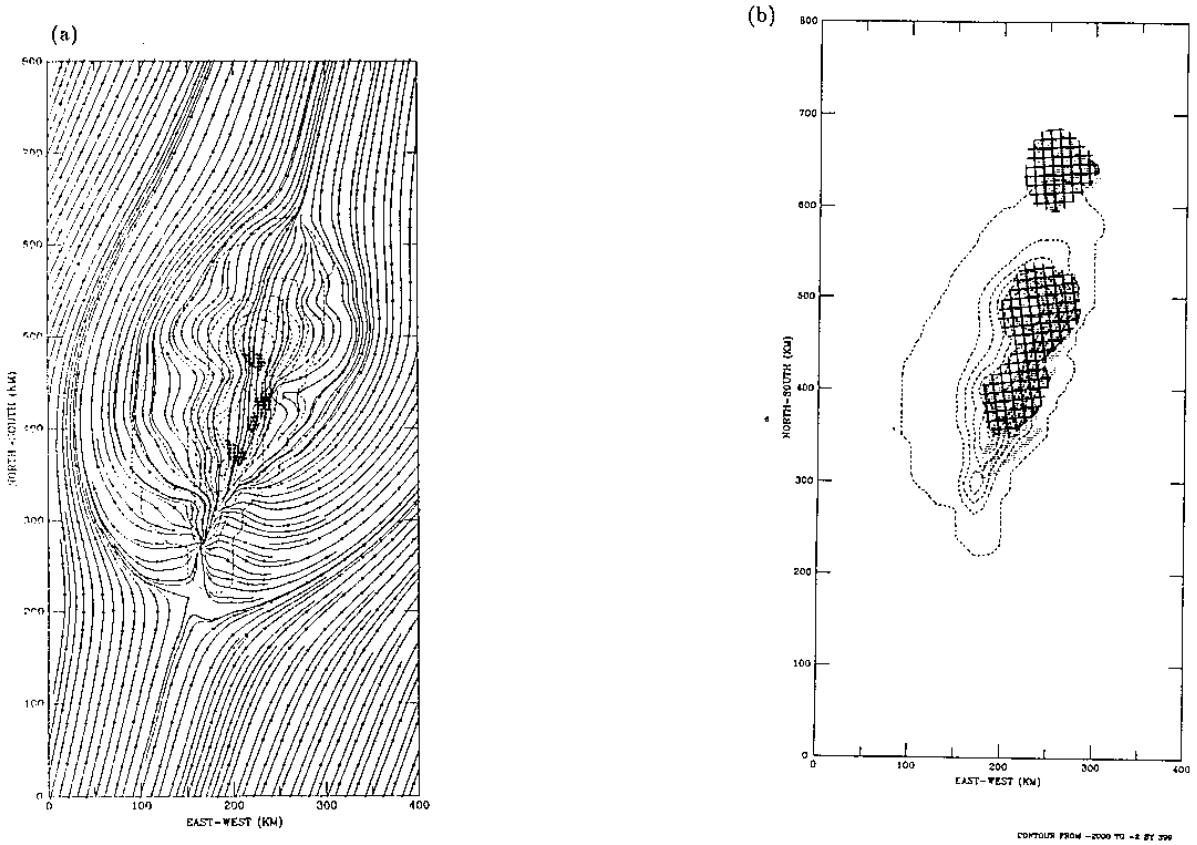


Fig. 14 Same as in Fig.9 but for June 20, 1987.